Hsa_circ_0094606 promotes malignant progression of prostate cancer by inducing M2 polarization of macrophages through PRMT1-mediated arginine methylation of ILF3

Yuwei Zhang[a,b†], Ke Wang[c†], Delin Yang[d†], Fengping Liu[b,e†], Xinyu Xu[b], Yangkun Feng[a], Yang Wang[b], Sha Zhu[f], Chaoqun Gu[a], Jiayi Sheng[b], Lei Hu[b], Bin Xu[g*], Yong-Jie Lu[h*], Ninghan Feng[a,b*]

[a]Medical College of Nantong University, Nantong, China

[b]Department of Urology, Affiliated Wuxi No.2 Hospital, Nanjing Medical University, Wuxi, China

[c]Department of Urology, The Affiliated Hospital of Qingdao University, Qingdao, China

[d]Department of Urology, Second Affiliated Hospital of Kunming Medical University, Kunming, China

[e]Wuxi School of Medicine, Jiangnan University, Wuxi, China

[f]Department of Oncology, Affiliated Wuxi No.2 Hospital, Nanjing Medical University, Wuxi, China

[g]Department of Urology, Affiliated Zhongda Hospital of Southeast University, Nanjing, China

[h]Centre for Biomarkers and Biotherapeutics, Barts Cancer Institute, Queen Mary University of London, John Vane Science Building Charterhouse Square, London, UK

[†] **These authors contributed equally to this work.**

* **Correspondence:**

Ninghan Feng, MD, PhD, Professor, Medical College of Nantong University, 9 Qiangyuan Road, Nantong, 226019, China. Telphone: +8613861892528, E-mail: n.feng@njmu.edu.cn

Yong-Jie Lu, MD, PhD, Professor, Centre for Biomarkers and Biotherapeutics, Barts Cancer Institute, Queen Mary University of London, John Vane Science Building Charterhouse Square, London, UK. EC1M 6BQ. Tel: 020 7882 3597. Email: y.j.lu@qmul.ac.uk

And Bin Xu, MD, Professor, Department of Urology, Affiliated Zhongda Hospital of Southeast University, 87 Dingjia Bridge Hunan Road, Nanjing, 210009, China. Tel: +8618012949196. E-mail: njxbseu@seu.edu.cn

Abstract

Circular RNA (circRNA), a type of noncoding RNAs, has been demonstrated to act vital roles in tumorigenesis and cancer deterioration. While tumor-associated macrophages (TAMs) involved in tumor malignancy, the interactions between circRNAs and TAMs in prostate cancer (PCa) remains unclear. In the present study, we found that hsa_circ_0094606 (subsequently named circ_0094606) could promote proliferation, epithelial mesenchymal transition (EMT) as well as migration of PCa cells through cell viability and migration assays and the determination of EMT markers. Mass spectrometry analysis after RNA pull-down experiment identified that circ_0094606 bound to PRMT1 in PCa cells, and further functional assays revealed that circ_0094606 promoted malignant progression of PCa by binding to PRMT1. Moreover, Co-IP, GST pull-down and Immunofluorescence showed that PRMT1 mediated arginine methylation of ILF3 to stabilize the protein. Bioinformatics analysis combined with data from RIP and RNA-pull down suggested that ILF3 could stabilize IL-8 mRNA, which promoted the M2 polarization in co-culture study. Finally, *in vivo* experiments showed that circ_0094606 subserve PCa growth and promoted the M2 polarization of macrophages through the PRMT1/ILF3/IL-8 regulation pathway, supporting circ_0094606 as a potential novel effective target for PCa treatment.

Keywords: hsa_circ_0094606; PRMT1; ILF3; M2 polarization; prostate cancer

Graphical abstract

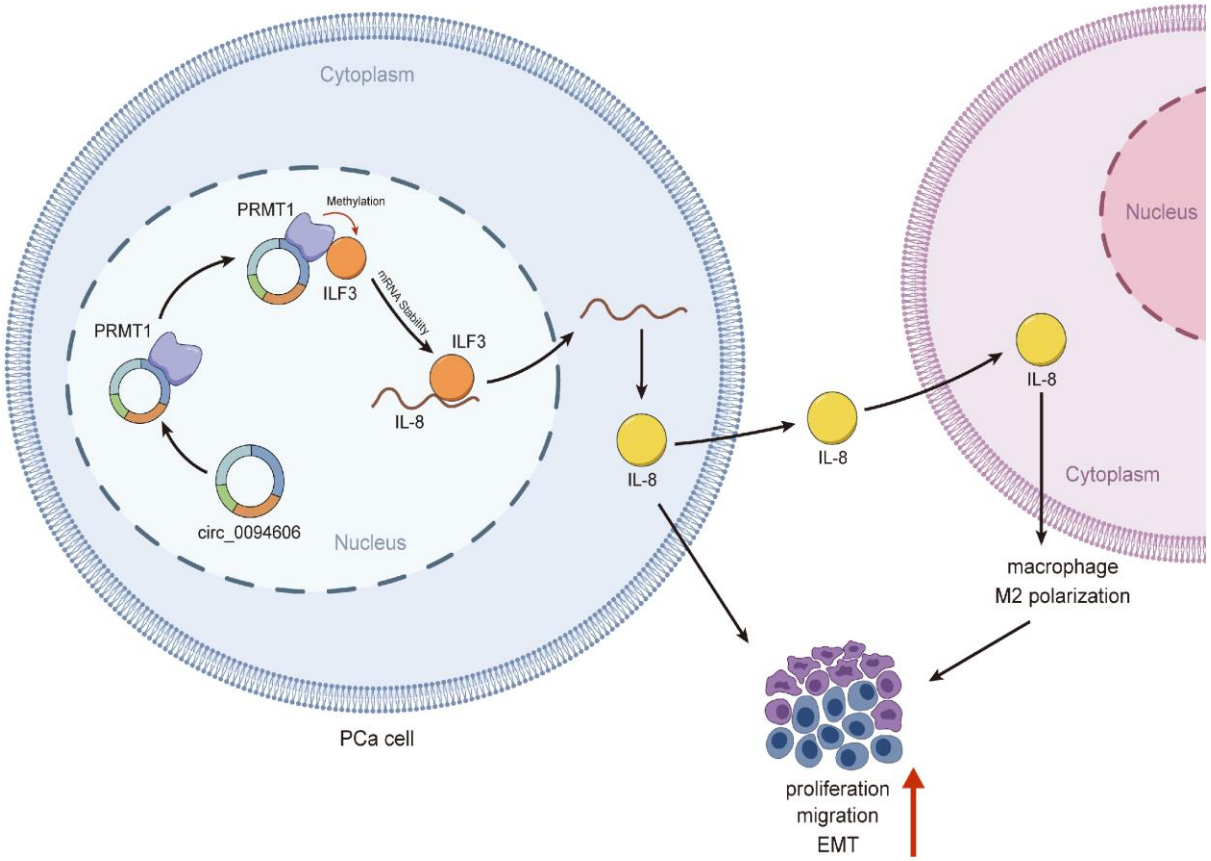

Introduction

Prostate cancer (PCa), the second most common cancer of the male worldwide, over one million people suffer from which every year[1]. The incidence and mortality rates of PCa have risen significantly worldwide, and the overall incidence rate is currently in the fourth place, after cancers of the breast, lung, and colorectum[1]. Because PCa has a high dependence on androgens, androgen deprivation therapy (ADT) has been an efficient treatment that, in most cases, inhibits tumor progression. However, resistance to the treatment inevitably occurs, eventually developing into castration-resistant prostate cancer (CRPC)[2-4]. Although previous studies reported several molecular biomarkers of PCa progression, little is known about tumor microenvironment in which these molecular biomarkers may contribute to the development of CRPC.

Up to now, the worth of noncoding RNAs (ncRNAs) in the deterioration of PCa has earned more and more attention[5]. Circular RNA (circRNA), derived from precursor mRNA, can be classified by composition into ecircRNAs containing only exons, ciRNAs composing only introns and EIciRNAs consisting of both, among which ecircRNAs account for over 80% discovered circRNAs[6-8]. CircRNAs specifically structured as a covalently closed-loop, leading to a higher stability than that of linear RNA[9], making them more stable and resistant to degradation of RNA enzymes, such as RNase R[10], and suitable tumor markers[11]. Several researches have identified that circRNAs modulate mRNAs through the competitive endogenous RNA (ceRNA) network in the cancer development[12]. Recent studies have reported that a few circRNAs can bind to RNA-binding proteins (RBPs) in the development of cancers[13]. Previous researches have elucidated that a variety of circRNAs are involved in the development of tumors and thought to be biomarkers and therapy targets of cancers[14-16]. However, studies of circRNAs in PCa are scarce.

Protein arginine methyltransferase 1 (PRMT1) is a member of the family of protein arginine methyltransferases (PRMTs). Previous studies have clarified that PRMT1 catalyzes asymmetric dimethylation of histone H4 on arginine 3 (H4R3me2a), which is often considered a marker of transcriptional activation[17]. In addition to transcriptional control, PRMT1 also plays a vital role in

precursor mRNA splicing, protein stability and DNA damage repair[18]. PRMT1 is involved in various interactions between transcription factors and promoters, and aberrant PRMT1 expression has been reported to directly affect tumourigenesis of the breasts and lungs as well as white blood cells[19-22]. However, the roles of PRMT1 in PCa progression have not been reported yet, and its relationship with circRNAs warrants further exploration.

Macrophages are one of the most abundant immune subgroups in various solid tumors and play vital roles in tumor microenvironment[23]. The phenotype and functions of macrophages are regulated by surrounding environment, a phenomenon called macrophage polarization. Polarized macrophages can be divided into pro-inflammatory M1 type and antagonistic M2 type, of which, M2 macrophages promote cancer development and progression[24]. Different polarizations of macrophages can be affected by ncRNAs[25], but the potential molecular mechanism remains elucidation.

In the present study, we illustrated that circ_0094606 is up-regulated in PCa cells, and the elimination of circ_0094606 can weaken proliferation and migration of PCa cells. Mechanistically, circ_0094606 binds to PRMT1 and promotes the M2 polarization of macrophages to subserve PCa development by stabilizing ILF3 and upregulating IL-8.

Materials and Methods

Ethical statement and sample acquirement. Forty-one PCa specimens and their paired non-tumor tissues were acquired from patients at Wuxi No. 2 Hospital affiliated with Nanjing Medical University. All patients received no endocrine therapy before surgery, and all patients underwent radical prostatectomy. The samples were preserved with liquid nitrogen. The Ethics Committee authorized this project (2021-Y-79) .

Cell culture. Human prostate cancer cell lines (i.e., DU145, PC3, NCI-H660) and normal human prostate cell line (i.e., RWPE-1) were acquired from iCell Bioscience Inc (Shanghai, China) in February 2021. All cell lines used in this study were tested and authenticated by DNA sequencing using the STR method (ABI 3730XL Genetic Analyzer) and tested for the absence of mycoplasma contamination (MycoAlert). The latest test was in December 2020. RPMI 1640 medium (Gibco,

USA) mixed with 10% fetal bovine serum (BI, Israel), and 1% penicillin/streptomycin (Gibco, USA) was used to culture all cell lines at 37℃ in a 5% CO_2 atmosphere.

RNA isolation and quantitative real-time PCR (qRT-PCR). Trizol Regent (Invitrogen, USA) was utilized to isolate total RNA. HiScript III RT SuperMix (Vazyme, China) was used to perform the reverse transcription for mRNAs and circRNAs. qRT-PCR was used to analyze the expression level of mRNAs and circRNAs, which was performed by SYBR Green Kit (Yeasen, China) using LightCycler® 96 SW 1.1 system (Roche, Switzerland). β-actin was considered as an endogenous control. As described in the instructions, the qRT-PCR experiment was carried out in three steps. In the first step, predenaturation reaction was carried out at 95℃ for 5 min. The second step has 40 cycles. Each cycle has denaturated reaction at 95℃ for 10 s, followed by annealing and extension reaction at 60℃ for 30 s. The third step is the determination of melting reaction, including reactions at 95℃ for 15 s, at 60℃ for 60 s, and finally at 95℃ for 15 s. The value of comparative cycle threshold (2-ΔΔCT) was analyzed to determine expression outcomes. All the sequences of oligos can be seen in Supplementary Table 1. Every qRT-PCR experiment was carried out for three replicates.

Western blot assay. RIPA (Beyotime, China) mixed with a protease inhibitor (Beyotime) was used to extract total cell protein. The protein concentration level was detected with the BCA kit (Beyotime). The proteins were separated, and then transfered to a polyvinylidene difluoride (PVDF) membrane, which was further soaked in 10% milk for one hour and a half. Subsequently, the membrane was soaked in the primary antibody (1:1000, Abcam, USA) of the protein for 12 h, and was then treated with the matched secondary antibody (1:5000, Abcam) at room temperature (RT) for 1 h. Ultimately, enhanced chemiluminescence (Tanon, China) was used to detect the blot. Every Western blot assay was carried out for three replicates.

Lentivirus and plasmids transfection. The lentivirus to suppress circ_0094606, PRMT1 as well as ILF3, and the plasmids to overexpress PRMT1 as well as ILF3 were synthesized by Ribobio (Guangdong, China). Indicated cells were infected with the viral particles in line with the manufacturer's instructions. Plasmids were transfected with Lipo3000 (Invitrogen, USA) in term of the instruction manual.

RNase R and Actinomycin D (Act D) treatment assay. Indicated cells planted in a six-well plate were incubated with 5 μg/ml Act D and harvested at indicated time point after 24 h when the confluence reached 70%. Total RNA (2 μg) and 3 U/μg RNase R (Lucigen, USA) were kept at 37℃ for 15 min. Finally, the circ_0094606 expression level was analyzed by qRT-PCR. Each experiment was performed for three replicates.

Cell counting kit-8 (CCK8) and clone formation experiment. 3×10^3 PCa cells were seeded into 96-well plates and were cultured for indicated time points. In each time point, 10 μL of CCK8 reagent (Yeasen) was mixed with cells for another 1 h. Eventually, the OD values were measured at 450 nm.

As for clone formation experiment, 1000/well of indicated cells were cultured in an atmosphere of 5% CO_2 at 37℃ for 2 weeks. Finally, methanol and crystal violet were used to fix and stain cells, respectively. Each experiment was performed for three replicates.

Transwell assay. Cell migration assay was performed with 24-well no-matrigel Transwell chambers (Corning, USA). 8×10^4 PC3 or DU145 cells were cultured in the upper chamber suspending in 200 μL medium without FBS, and the bottom chamber was added with 650 μL RPMI-1640 containing 10% FBS.

Furthermore, to detect the influence of M2 macrophages induced by circ_0094606, 1×10^4 macrophages were added into the bottom 24-well plate in 600 μL medium with 10% FBS and 2×10^4 PC3 cells were co-cultured into the upper chamber. After overnight incubation, crystal violet was used to stain the cells on the lower surface of the chamber for 20 min. Eventually, images of three random fields were acquired using a fluorescence microscope, and then the cells were calculated. Each experiment was performed for three replicates.

Wound healing experiment. Indicated cells were planted in 6-well plates, and equidistant marks were drawn with a pipette tip. After culturing in the medium without FBS for 24 h, the pictures of cells were acquired. Each experiment was performed for three replicates.

Flow cytometry. Indicated cells were collected and centrifuged at 350g for 5 min. PBS was used to wash the pellet twice. 3% BSA was mixed to each sample at 4℃ for 15 min for blocking. 1 μl of $CD206^+$ or $CD86^+$ antibodies were mixed with 100 μl cell suspension and stained at room temperature in dark for 20 min. Final results were analyzed using the Flowjo software (Tree Star, USA) . Each experiment was performed for three replicates.

Fluorescence in situ hybridization (FISH) assay. The probe of circ_0094606 was acquired from GenePharma (China). Indicated cells were fixed and then washed by PBS and treated with RNase R for 15 min. The cell suspension was transferred to a glass slide, and then dehydrated with a gradient of ethanol. Subsequently, hybridization was ongoing overnight in a humid and dark atmosphere. The sections were washed twice with 50% formamide/2 × SSC for a total of 10 min, then treated with Alexa FluorTM 488 Tyramide SuperBoost™ Kits (Thermo, USA) for 30 min, and finally sealed with a parafilm mixed with DAPI. A fluorescence microscope was used to acquire images. Each experiment was performed for three replicates.

Macrophage polarization experiment. PC3 cells were co-cultured with macrophages, and macrophage surface maker CD86 (M1 label) as well as CD206 (M2 label) were determined by flow cytometry (BD Biosciences). Each experiment was performed for three replicates.

RNA pull-down assay and mass spectrometry analysis. The specific probe of circ_0094606 was acquired from GenePharma (China). The probe was treated with extracts from indicated cells at RT for 2 h and incubated with 35 μl of Streptavidin C1 magneticbeads (Invitrogen) for 1 h. The proteins were then analyzed by mass spectrum assay (Bioprofile, China).

RNA-binding protein immunoprecipitation (RIP) assay. This assay was performed abiding by the protocol of Magna RIP Kit (Millipore, USA). In short, indicated cells were harvested 48 h after transfection and lysed for 30 min. Subsequently, the supernatant was centrifugated and then treated with 30 μl magnetic beads and indicated antibodies. The immune complex, incubated overnight, was centrifuged and washed five times with washing buffer. Western blot was performed to identify the bead binding protein, and qRT-PCR was carried out to analyze the immunoprecipitated RNA. Each experiment was performed for three replicates.

Immunohistochemistry (IHC) staining. The tissue was sequentially fixed, dehydrated, paraffin-embedded, and sliced at 4 μm. The slides were deparaffinized, rehydrated and mixed with 3% H_2O_2. After antigen retrieval and blocking, the sections were soaked in indicated antibodies (1:200) (Abcam, USA) overnight. The sections were subsequently treated with the matched antibody for 30 min at RT, then treated with the streptavidin peroxidase complex, and further stained with 3,3-Diaminobenzidine (DAB) substrate kit. Eventually, a light microscope was used to acquire images. Each experiment was performed for three replicates.

Luciferase reporter experiment. The IL-8 promoter sequence and 3'UTR sequence were cloned into the p-GLO Dual-Luciferase vector (Vigenebio, USA). Indicated cells were cultured with a density of 40% overnight before transfection and co-transfected with 800 ng p-GLO dual luciferase reporter gene, 1 ng ILF3 plasmid and its control plasmid. Forty-eight hours later, the relative luciferase activity was detected. Each experiment was performed for three replicates.

In vivo experiments. The Institutional Animal Care and Use Committee of Nanjing Medical University authorized the animal experiments (IACUC-2109015). Six healthy 6-week-old BALB-C nude mice with control weights between 20-23 g were randomly separated into 2 teams of 3 mice each. Approximately 1×10^7 PC3 cells washed with PBS were injected subcutaneously in the same area of the back of each mouse at one time while the mice were in good condition. Starting from 7 d after injection, mice were observed every 3 d and the volume of xenografts was recorded. After 28 d of injection, all the mice were executed under general anesthesia (induced with an intraperitoneal injection of pentobarbital sodium (150 mg/kg)) and the tumors were removed for subsequent analyses.

Statistical analysis. Data were presented as the mean ± SD. Paired or nonpaired 2-tailed t-test was used for comparisons between 2 groups. R software (version 4.1.0) was used for statistical analysis. $P < 0.05$ was considered significant.

Results

Characterization of circ_0094606 in PCa cells.

To investigate circRNA alterations in PCa, we carried out a circRNA sequencing using one pair of PCa and corresponding non-tumor tissues, and hsa_circ_0094606 (next called circ_0094606) was identified to be expressed at the highest level in PCa tissue (**Figure. 1A, 1B**). Subsequently, we made

a comparison between the expression of circ_0094606 in tumor tissues and that in matched normal tissues from 40 PCa patients, and we found that the expression of circ_0094606 was high in 70% of PCa patients (**Figure. 1C, 1D**). qRT-PCR analyses in normal human prostate epithelial cell line RWPE-1 and three PCa cell lines including PC3, DU145 and NCI-H660 were further performed. Results revealed that compared to RWPE-1, the abundance of circ_0094606 was markedly elevated in PCa cells particularly in PC3 and DU145 (**Fig. 1E**), which we chosen for the further experiments. Circ_0094606 is back-spliced from 4 exons (exons 24-27) of the *SORBS1* gene and the loop structure was confirmed by Sanger sequencing (**Figure. 1F**). The circular structure of circ_0094606 was confirmed, since it could only be amplified by divergent primer in cDNA (**Fig. 1G**) and be resistant to RNase R or ActD treatment (**Fig. 1H-I**). In the meantime, we identified the localization of circ_0094606 in the cytoplasm and nucleus of both DU145 and PC3 cells (**Fig. 1J-K**). In general, these results illustrated that circ_0094606 is an abundant and stable circRNA expressed in PCa.

Circ_0094606 promotes the proliferation, migration and EMT progression of PCa cells.

To detect the impact of circ_0094606 on PCa cell functions, we attempted to knockdown circ_0094606 in PCa cells. All the three sh-circ_0094606 tested achieved > 50% knockdown of expression level of circ_0094606 (**Supplementary Fig. 1A**) and we chose the two sh-circ_0094606 with better knockdown effect for further functional analysis. When circ_0094606 was inteferenced, the proliferation and migration of PCa cells were significantly reduced (**Supplementary Fig. 2A-D**). Meanwhile, cell morphology changed from a spindle shape to a round shape under circ_0094606 interference (**Supplementary Fig. 2E**), indicating that the cells were less invasive. Epithelial-mesenchymal transition (EMT) has close relation to the migration and invasion capabilities of tumor cells[26]. Therefore, we measured protein markers involved in the EMT process with circ_0094606 knockdown in PCa cells. And the results revealed that the expression of epithelial cell marker ZO-1 and E-cadherin was up-regulated when weakening circ_0094606, while the levels of mesenchymal cell marker N-cadherin and Vimentin were down-regulated in both PC3 and DU145 cells under such a

circumstance (**Supplementary Fig. 2F**). Overall, circ_0094606 was positively correlated with aggressive phenotypes of PCa cells.

Circ_0094606 promotes the malignant progression of PCa by binding to PRMT1.

Subsequently, we investigated the molecular mechanism by which circ_0094606 promotes PCa development. We carried out the pull-down experiment with the probe targeting circ_0094606. In performing mass spectrometry[27], we identified 574 proteins that could bind to circ_0094606 (**Supplementary Table 2**). We focused on the top thirty proteins in order of the PEP score and finally selected the protein arginine methyltransferase 1 (PRMT1), which was highly enriched by biotinylated circ_0094606 (**Supplementary Fig. 3**), as the focus of our study through literature analysis.

Arginine methylation is reported as a post-translational modification[28], and PRMT1 plays vital roles in the progression of a variety of tumors[29-31]. In addition, we interfered the PRMT1 expression in PCa cells (**Supplementary Fig. 1B**) and identified that PRMT1 could facilitate the proliferation, migration and EMT of both PC3 and DU145 through loss-of-function experiments (**Supplementary Fig. 4**).

To validate the circ_0094606 - PRMT1 interaction, we performed RIP experiments and RNA pull-down experiments in both PC3 and DU145 cells (**Fig. 2A-B** and **Supplementary Fig. 5A-B**). Furthermore, the co-localization of circ_0094606 and PRMT1 was identified by FISH and IF in both two PCa cell lines (**Fig. 2C** and **Supplementary Fig. 5C**). Like circ_0094606, PRMT1 was also found to be expressed at high levels in PCa cells relative to RWPE-1 (**Fig. 2D-E**). Then, we up-regulated PRMT1 in PCa cells through transfecting with pcDNA3.1-PRMT1 (**Supplementary Fig. 1C**). Importantly, overexpression of PRMT1 could rescue the proliferation and migration capacities impaired by knocking down circ_0094606 (**Fig. 2F-G** and **Supplementary Fig. 5D-G**). In conclusion, we identified that circ_0094606 promotes the malignant progression of PCa by binding to PRMT1.

PRMT1 mediates ILF3 methylation at R609 site.

PRMT1 is known as an arginine methyltransferase to regulate target protein methylation and therefore affect cancer progression. Hence, searching the downstream target protein of PRMT1 in PCa cells was necessary. We first predicted the proteins that might bind to PRMT1 using HitPredict database. Screening proteins with a score of 0.65 or higher as candidates, we identified FUS, ROA1, KHDR1, HNRPK, ER300, CDC37 and ILF3 based on scoring in a descending order (**Fig. 3A**). The results of further co-immunoprecipitation (co-IP) experiments performed with PC3 cells showed that ILF3 bound most tightly to PRMT1 (**Fig. 3B**). Additionally, we verified the co-localization of ILF3 and PRMT1 in the nucleus of two kinds of PCa cells (**Fig. 3C** and **Supplementary Fig. 6A**). To verify the precise methylation site in ILF3 by PRMT1, we applied GST-pull down assays via different ILF3 fragments. Results indicated that the sites of 601-650 were responsible for the recognition by PRMT1 (**Fig. 3D**). Then, we tested the influence of PRMT1 on ILF3. qRT-PCR results revealed that the mRNA level of ILF3 was almost unaffected in response to PRMT1 interference (**Fig. 3E** and **Supplementary Fig. 6B**). However, ILF3 protein expression decreased significantly with PRMT1 interference (**Fig. 3F** and **Supplementary Fig. 6C**). Subsequently, we performed Western blot experiment in PC3 cells to identify the alterations in the expression level of ILF3 after overexpression of PRMT1. The outcomes revealed that the protein expression of ILF3 increased after overexpression of PRMT1. Further addition of the arginine methylation inhibitor MS023 reversed this result, demonstrating that PRMT1 mediated arginine methylation of ILF3 (**Fig. 3G** and **Supplementary Fig. 6D**).

In order to identify which site was methylated by PRMT1 in ILF3, we searched the PhosphoSitePlus database and found that ILF3 had a highly probable methylation site at the arginine position 609 (**Supplementary Fig. 6E**). We then constructed HA-ILF3 WT and HA-ILF3 R609K (replacing the arginine at position 609 of ILF3 with lysine) mutant plasmids. It manifested that R609 mutation in ILF3 decreased its methylation level induced by PRMT1 (**Fig. 3H** and **Supplementary Fig. 6F**).

Furthermore, Co-IP results suggested that R609 mutation in ILF3 hampered its methylation modified by PRMT1 (**Fig. 3I** and **Supplementary Fig. 6G**). In summary, all the above experiments illustrated that PRMT1 mediates ILF3 methylation at R609.

ILF3 R609 methylation enhances PCa cell proliferation, migration and EMT processes.

Next, we aimed to identify the effect of ILF3 methylation on PCa cell functions. Before that, we analyzed the function of ILF3 in PCa cells. After confirming the knockdown of ILF3 in PCa cells (**Supplementary Fig. 1D**), we discovered that silencing ILF3 markedly impeded proliferation, migration and EMT of PCa cells (**Supplementary Fig. 7A-F**). Interestingly, results showed that the proliferation and migration of PCa cells transfected with ILF3 R609K plasmid were significantly reduced, compared to those transfected with ILF3 WT plasmid (**Supplementary Fig. 8A-D**). At the same time, we observed that PCa cells transfected with ILF3 R609K plasmid were equipped with rounder shapes than those treated with ILF3 WT (**Supplementary Fig. 8E**), suggesting that the invasion ability of the cells was decreased. Analysing EMT markers, we identified that contrasted with the ILF3 WT group, the epithelial cell markers (ZO-1 and E-cadherin) expression was remarkably increased, while the mesenchymal cell markers (N-cadherin and Vimentin) expression was remarkably decreased in ILF3 R609K group (**Supplementary Fig. 8F**). All the above experiments illustrated that methylation of ILF3 at R609 can enhance the malignancy of PCa cells.

ILF3 binds to IL-8 mRNA to stabilize IL-8 expression.

ILF3 is an interleukin-enhanced binding factor that can affect the abundance of mRNAs involved in immune response[32]. It has also been documented that ILF3 can stabilize downstream mRNAs such as IL-8[33], which can promote proliferation and apoptosis inhibition in PCa via MAPK/ERK pathway[34]. In addition, previous studies identified that IL-8 is an immunomodulator that promotes M2

polarization in macrophages[35]. Therefore, we performed a series of experiments around these speculations.

We predicted the binding possibility of ILF3 to *IL-8* (CXCL8) mRNA using Starbase database (**Fig. 4A**). We then demonstrated the interaction between ILF3 and IL-8 using RIP and RNA pull-down experiments (**Fig. 4B-C** and **Supplementary Fig. 9A-B**). qRT-PCR and Western blot revealed that knockdown of ILF3 in PC3 cells led to a remarkably reduction of IL-8 in both mRNA and protein levels (**Fig. 4D-E** and **Supplementary Fig. 9C-D**). Then, we examined whether ILF3 could act on IL-8 mRNA at transcriptional or post-transcriptional level. As expected, the outcomes of dual luciferase reporter assays revealed that overexpression of ILF3 (validated in **Supplementary Fig. 1E**) led to remarkable reduction in the luciferase activity of IL-8 3'UTR but not IL-8 promoter (**Fig. 4F-G** and **Supplementary Fig. 9E-F**). Subsequently, we performed mRNA stability assays and the results showed that ILF3 could improve the stability of IL-8 mRNA (**Fig. 4H** and **Supplementary Fig. 9G**). Above all, these results suggested that ILF3 binds to IL-8 mRNA to stabilize its expression.

Circ_0094606 promotes M2 polarization of macrophages through the regulation of IL-8.

It has been reported that the up-regulation of IL-8 is correlated with increased microvessel density[36]. In addition, IL-8 can also promote macrophage M2 polarization, thereby promoting PCa immune escape and further accelerating malignant progression of PCa[35]. Based on our findings that circ_0094606 up-regulated IL-8 expression via PRMT1/ILF3 signaling in PCa cells, we speculated that circ_0094606 also played a role in regulating M2 polarization of macrophages in PCa.

We induced THP-1 cells to differentiate into macrophages using PMA, and then co-cultured PCa cells and macrophages for 48 h. Flow cytometry detected macrophage surface markers, and the results showed that the proportion of $CD14^+CD206^+$ macrophages (M2 macrophages) was lowered, while that of $CD14^+CD86^+$ macrophages (M1 macrophages) was elevated under circ_0094606 interference (**Fig. 5A-B**). Likewise, qRT-PCR results revealed that the expression level of macrophage M2 polarization markers (including IL4, CCL22 and ARG1) was significantly decreased, while that of

M1 polarization markers (including iNOS, TNF-α and TLR4) was significantly increased when co-culturing with circ_0094606-silenced PCa cells (**Fig. 5C-E**). All these results indicated that circ_0094606 can promote the M2 polarization of macrophages. Meanwhile, we found that with the knockdown of circ_0094606, the mRNA and protein levels of IL-8 in PCa cells were also decreased (**Fig. 5F-G**). Collectively, our results suggested that circ_0094606 promotes M2 polarization of macrophages through the regulation of IL-8.

Circ_0094606 contributes to in vivo tumorigenesis and macrophage M2 polarization in PCa.

Finally, in vivo experiments as detailed in Materials and Methods were carried out to further validate the role of circ_0094606 in PCa. As a result, tumors generated from PCa cells with circ_0094606 knockdown grew significantly slower than those in control group (**Fig. 6A**), resulting in smaller and lighter xenografts in such group than controls (**Fig. 6B-C**). Also, the expression level of Ki67 was lowered, and the EMT process was blocked in circ_0094606-difecient xenografts (**Fig. 6D-E**). Moreover, we found that the levels of both ILF3 and IL-8 were reduced in xenografts from circ_0094606-silenced group (**Fig. 6F**). The percentage of $CD14^+CD206^+$ M2 macrophages was also reduced, while that of $CD14^+CD86^+$ M1 macrophages was augmented in tumors with circ_0094606 knockdown (**Fig. 6G**), along with the same trends in the levels of M1/M2 markers in these xenografts (**Fig. 6H**). Altogether, circ_0094606 facilitates PCa cell growth and migration through promoting macrophage M2 polarization.

Discussion

In the present study, we identified that circ_0094606 was remarkably up-regulated in PCa cells. After knock-down of circ_0094606, the PCa cell proliferation, migration and EMT processes were severely attenuated. Mechanically, circ_0094606 could promote the deterioration of PCa by binding to PRMT1. Overexpression of PRMT1 could rescue the PCa cell diminished proliferation and migration

capacities caused by circ_0094606 interference. Meanwhile, PRMT1 could induce R609 methylation of ILF3 to improve the mRNA stability of IL-8. Ultimately, circ_0094606 could strengthen IL-8 expression to induce M2 polarization of macrophages to promote malignant progression of PCa.

Basic biological processes of gene transcription, splicing and cell metabolism alter in many diseases, which are reportedly regulated by protein arginine methyltransferase (PRMT)[37]. Therefore, PRMT has become an attractive therapeutic target. Understanding the mechanism by which these enzymes promote the malignant process of tumors, especially in a specific metabolic environment or in the presence of certain mutations, provides a theoretical basis for targeting them in therapy development. PRMT1 is the main catalytic enzyme in type I arginine methylation modification enzyme[38], present in 90% of mammalian cells, and can promote the methylation of multiple substrates in cells, such as transcription factor FOXO1, RNA junction protein SERBP1, histone protein H4R3 and DNA repair factor 53BP1[39]. One study[40] reported that A9 targeting PRMT1 remarkably impeded proliferation of castrate-resistant PCa cells. To our best know, we are the first to identify the circRNA – PRMT1 interaction, and our study provided the first-hand evidence that circ_0094606 bound to PRMT1 to promote the development of PCa.

Macrophages participate in tissue homeostasis to promote or subside inflammation, cause tissue damage or help tissue repair[41]. A growing amount of evidence has shown that macrophage polarization is a dynamic process that can be reversed and modified, which is involved in the development of many immune inflammatory diseases and tumors[42]. Reversing the polarization state of macrophages is considered a new strategy for developing tumor therapy. In the present study, we innovatively discovered that circ_0094606 could bind to PRMT1 and mediate R609 methylation of ILF3, resulting in an enhanced stability of IL-8 mRNA. Meanwhile, IL-8 could induce the M2 polarization of macrophages, which may accelerate PCa growth, but yet to be confirmed in future studies.

So far, three mechanisms for circRNA to exert its biological functions in tumors have been studied in depth. The first is the most widely reported regulatory mechanism by competing endogenous RNAs

(ceRNA); that is, circRNA can act as a miRNA sponge for its binding site to regulate downstream target genes. The second is that few of circRNAs are thought to function by translating micropeptides[26]. The third is that part of circRNAs can regulate gene expression at the post-transcriptional level[43]. In the present study, we clarified an effective mechanism, that is, circ_0094606 could promote the methylation of ILF3 R609 by binding to PRMT1 protein to further increase the stability of IL-8 mRNA.

More interestingly, we are the first to identified that circ_0094606 induced the malignant process of PCa by influencing TAMs. The clarification of a close connection between circRNA and tumor microenvironment in PCa is of great importance, which may help open some new approaches to the diagnosis and treatment of PCa.

Acknowledgements

This study was supported by the National Natural Science Foundation of China (SQ2017YFSF090096, 81872089), Natural Science Foundation of Jiangsu Province (BE2019751), Jiangsu Provincial Medical Talent (ZDRCA2016080), Key R & D (Social Development) Projects of Jiangsu Province (BE2018629) and Wuxi "Taihu Talents Program" Medical and Health High-level Talents Project. We appreciate Shanghai Bioprofile Technology Company Ltd for technological assistance in mass spectrometry assay.

Author contributions

Ninghan Feng, Yong-jie Lu, and Bin Xu designed this study and provided clinical guidance as well as data interpretation. Yuwei Zhang, Ke Wang, Deling Yang and Fengping Liu performed the experiments. Xinyu Xu, Yangkun Feng and Yang Wang prepared the figures for this study. Sha Zhu, Chaoqun Gu, Jiayi Sheng and Lei Hu checked the data. Yuwei Zhang drafted the article. All authors reviewed the manuscript, provided comments and approved the final version.

Ethical Approval

This study was approved by the Ethics Committee of Wuxi No. 2. Hospital affiliated with Nanjing Medical University (2021-Y-79).

Competing Interests

The authors report no conflict of interest.

Data Availability Statement

The data of this study are available from the corresponding author on reasonable request.

References

1. Sung H, Ferlay J, Siegel RL, Laversanne M, Soerjomataram I, Jemal A, et al. Global Cancer Statistics 2020: GLOBOCAN Estimates of Incidence and Mortality Worldwide for 36 Cancers in 185 Countries. *CA Cancer J Clin* 2021; **71**(3): 209-49.
2. Orme JJ, Huang H. Microenvironment-Mediated Resistance to Anti-Androgen Therapy. *Cancer Cell* 2020; **38**(2): 155-7.
3. Rasool RU, Natesan R, Deng Q, Aras S, Lal P, Sander Effron S, et al. CDK7 Inhibition Suppresses Castration-Resistant Prostate Cancer through MED1 Inactivation. *Cancer Discov* 2019; **9**(11): 1538-55.
4. Lokeshwar SD, Klaassen Z, Saad F. Treatment and trials in non-metastatic castration-resistant prostate cancer. *Nat Rev Urol* 2021; **18**(7): 433-42.
5. Hua JT, Chen S, He HH. Landscape of Noncoding RNA in Prostate Cancer. *Trends Genet* 2019; **35**(11): 840-51.
6. Kelly S, Greenman C, Cook PR, Papantonis A. Exon Skipping Is Correlated with Exon Circularization. *J Mol Biol* 2015; **427**(15): 2414-7.
7. Wilusz JE. Circular RNAs: Unexpected outputs of many protein-coding genes. *RNA Biol* 2017; **14**(8): 1007-17.
8. Cui X, Wang J, Guo Z, Li M, Li M, Liu S, et al. Emerging function and potential diagnostic value of circular RNAs in cancer. *Mol Cancer* 2018; **17**(1): 123.
9. Chen LL. The expanding regulatory mechanisms and cellular functions of circular RNAs. *Nat Rev Mol Cell Biol* 2020; **21**(8): 475-90.
10. Kristensen LS, Andersen MS, Stagsted LVW, Ebbesen KK, Hansen TB, Kjems J. The biogenesis, biology and characterization of circular RNAs. *Nat Rev Genet* 2019; **20**(11): 675-91.
11. Beermann J, Piccoli MT, Viereck J, Thum T. Non-coding RNAs in Development and Disease: Background, Mechanisms, and Therapeutic Approaches. *Physiol Rev* 2016; **96**(4): 1297-325.
12. Wang L, Zhou Y, Jiang L, Lu L, Dai T, Li A, et al. CircWAC induces chemotherapeutic resistance in triple-negative breast cancer by targeting miR-142, upregulating WWP1 and activating the PI3K/AKT pathway. *Mol Cancer* 2021; **20**(1): 43.
13. Okholm TLH, Sathe S, Park SS, Kamstrup AB, Rasmussen AM, Shankar A, et al. Transcriptome-wide profiles of circular RNA and RNA-binding protein interactions reveal effects on circular RNA biogenesis and cancer pathway expression. *Genome Med* 2020; **12**(1): 112.
14. Yang L, Zou X, Zou J, Zhang G. Functions of circular RNAs in bladder, prostate and renal cell cancer (Review). *Mol Med Rep* 2021; **23**(5).
15. Zhou H, Zheng XD, Lin CM, Min J, Hu S, Hu Y, et al. Advancement and properties of circular RNAs in prostate cancer: An emerging and compelling frontier for discovering. *Int J Biol Sci* 2021; **17**(2): 651-69.
16. Fang J, Qi J, Dong X, Luo J. Perspectives on Circular RNAs as Prostate Cancer Biomarkers. *Front Cell Dev Biol* 2020; **8**: 594992.
17. Tang M, Yang M, Wu G, Mo S, Wu X, Zhang S, et al. Epigenetic Induction of Mitochondrial Fission Is Required for Maintenance of Liver Cancer-Initiating Cells. *Cancer Res* 2021; **81**(14): 3835-48.
18. Hwang JW, Cho Y, Bae GU, Kim SN, Kim YK. Protein arginine methyltransferases: promising targets for cancer therapy. *Exp Mol Med* 2021; **53**(5): 788-808.
19. Liu LM, Sun WZ, Fan XZ, Xu YL, Cheng MB, Zhang Y. Methylation of C/EBPalpha by PRMT1 Inhibits Its Tumor-Suppressive Function in Breast Cancer. *Cancer Res* 2019; **79**(11): 2865-77.
20. Choucair A, Pham TH, Omarjee S, Jacquemetton J, Kassem L, Tredan O, et al. The arginine methyltransferase PRMT1 regulates IGF-1 signaling in breast cancer. *Oncogene* 2019; **38**(21): 4015-27.
21. He L, Hu Z, Sun Y, Zhang M, Zhu H, Jiang L, et al. PRMT1 is critical to FEN1 expression and drug resistance in lung cancer cells. *DNA Repair (Amst)* 2020; **95**: 102953.
22. Zhu Y, He X, Lin YC, Dong H, Zhang L, Chen X, et al. Targeting PRMT1-mediated FLT3 methylation disrupts maintenance of MLL-rearranged acute lymphoblastic leukemia. *Blood* 2019; **134**(15): 1257-68.
23. Ricketts TD, Prieto-Dominguez N, Gowda PS, Ubil E. Mechanisms of Macrophage Plasticity in the Tumor Environment: Manipulating Activation State to Improve Outcomes. *Front Immunol* 2021; **12**: 642285.
24. Mantovani A, Marchesi F, Malesci A, Laghi L, Allavena P. Tumour-associated macrophages as treatment targets in oncology. *Nat Rev Clin Oncol* 2017; **14**(7): 399-416.
25. Mohapatra S, Pioppini C, Ozpolat B, Calin GA. Non-coding RNAs regulation of macrophage polarization in cancer. *Mol Cancer* 2021; **20**(1): 24.
26. Pan Z, Cai J, Lin J, Zhou H, Peng J, Liang J, et al. A novel protein encoded by circFNDC3B inhibits tumor progression and EMT through regulating Snail in colon cancer. *Mol Cancer* 2020; **19**(1): 71.

27. Cho WC. Mass spectrometry-based proteomics in cancer research. *Expert Rev Proteomics* 2017; **14**(9): 725-7.
28. Zhao J, O'Neil M, Vittal A, Weinman SA, Tikhanovich I. PRMT1-Dependent Macrophage IL-6 Production Is Required for Alcohol-Induced HCC Progression. *Gene Expr* 2019; **19**(2): 137-50.
29. Yao B, Gui T, Zeng X, Deng Y, Wang Z, Wang Y, et al. PRMT1-mediated H4R3me2a recruits SMARCA4 to promote colorectal cancer progression by enhancing EGFR signaling. *Genome Med* 2021; **13**(1): 58.
30. Li Z, Wang D, Lu J, Huang B, Wang Y, Dong M, et al. Methylation of EZH2 by PRMT1 regulates its stability and promotes breast cancer metastasis. *Cell Death Differ* 2020; **27**(12): 3226-42.
31. Repenning A, Happel D, Bouchard C, Meixner M, Verel-Yilmaz Y, Raifer H, et al. PRMT1 promotes the tumor suppressor function of p14(ARF) and is indicative for pancreatic cancer prognosis. *EMBO J* 2021: e106777.
32. Vrakas CN, Herman AB, Ray M, Kelemen SE, Scalia R, Autieri MV. RNA stability protein ILF3 mediates cytokine-induced angiogenesis. *FASEB J* 2019; **33**(3): 3304-16.
33. Chan TW, Fu T, Bahn JH, Jun HI, Lee JH, Quinones-Valdez G, et al. RNA editing in cancer impacts mRNA abundance in immune response pathways. *Genome Biol* 2020; **21**(1): 268.
34. Kim J, Jin H, Zhao JC, Yang YA, Li Y, Yang X, et al. FOXA1 inhibits prostate cancer neuroendocrine differentiation. *Oncogene* 2017; **36**(28): 4072-80.
35. Kim JH. Interleukin-8 in the Tumor Immune Niche: Lessons from Comparative Oncology. *Adv Exp Med Biol* 2020; **1240**: 25-33.
36. Karashima T, Sweeney P, Slaton JW, Kim SJ, Kedar D, Izawa JI, et al. Inhibition of angiogenesis by the antiepidermal growth factor receptor antibody ImClone C225 in androgen-independent prostate cancer growing orthotopically in nude mice. *Clin Cancer Res* 2002; **8**(5): 1253-64.
37. Guccione E, Richard S. The regulation, functions and clinical relevance of arginine methylation. *Nat Rev Mol Cell Biol* 2019; **20**(10): 642-57.
38. Fong JY, Pignata L, Goy PA, Kawabata KC, Lee SC, Koh CM, et al. Therapeutic Targeting of RNA Splicing Catalysis through Inhibition of Protein Arginine Methylation. *Cancer Cell* 2019; **36**(2): 194-209 e9.
39. Jain K, Warmack RA, Debler EW, Hadjikyriacou A, Stavropoulos P, Clarke SG. Protein Arginine Methyltransferase Product Specificity Is Mediated by Distinct Active-site Architectures. *J Biol Chem* 2016; **291**(35): 18299-308.
40. Wang J, Chen L, Sinha SH, Liang Z, Chai H, Muniyan S, et al. Pharmacophore-based virtual screening and biological evaluation of small molecule inhibitors for protein arginine methylation. *J Med Chem* 2012; **55**(18): 7978-87.
41. Zhang W, Zhangyuan G, Wang F, Jin K, Shen H, Zhang L, et al. The zinc finger protein Miz1 suppresses liver tumorigenesis by restricting hepatocyte-driven macrophage activation and inflammation. *Immunity* 2021; **54**(6): 1168-85 e8.
42. Zhou W, Zhou Y, Chen X, Ning T, Chen H, Guo Q, et al. Pancreatic cancer-targeting exosomes for enhancing immunotherapy and reprogramming tumor microenvironment. *Biomaterials* 2021; **268**: 120546.
43. Li Z, Huang C, Bao C, Chen L, Lin M, Wang X, et al. Exon-intron circular RNAs regulate transcription in the nucleus. *Nat Struct Mol Biol* 2015; **22**(3): 256-64.

Figure legends

Fig. 1 Circ_0094606 with loop structure is highly-expressed in PCa cells. (A-B) Heatmap and volcano map of circ_0094606 in one pair of PCa tissue and corresponding normal tissue. (C) qRT‑PCR detected the circ_000094606 expression profile in 40 pairs of PCa tissues and corresponding normal tissues. (D) The expression of circ_0094606 was significantly high in 70% of PCa patients. (E) qRT-PCR detected circ_0094606 expression profile in PCa cell lines compared to normal RWPE-1 cells. (F) Genomic locus of circ_0094606 was detected by Sanger sequencing. Arrows act for divergent primers binding to the back-splicing site of circ_0094606. (G) Agarose gel electrophoresis tested the PCR products amplified by convergent or divergent primers in RWPE-1 cells. (H) qRT-PCR detected the effect of RNase R treatment on circ_0094606 and the linear SORBS1 mRNA. (I) qRT-PCR analyzed the levels of circ_0094606 and SORBS1 mRNA in DU145 cells under ActD treatment for indicated times. (J-K) FISH and nucleo-cytoplasmic separation experiments examined circ_0094606 distribution in PCa cells. *P<0.05. **P<0.01.

Fig. 2 Circ_0094606 contributes to the malignancies of PCa cells by binding to PRMT1. (A-B) RIP and RNA pull down experiments analyzed the interaction of PRMT1 and circ_0094606 in PC3 cells. (C) FISH and IF examined the co-localization of PRMT1 and circ_0094606 in PC3 cells. (D-E) qRT-PCR and Western blot detected the expression level of PRMT1 in PCa cell lines compared to normal RWPE-1 cells. (F-G) CCK-8 and transwell experiments examined PCa cell proliferation and migration abilities under different conditions. $^{**}P<0.01$.

Fig. 3 PRMT1 induces ILF3 methylation at R609 to enhance ILF3 level in PCa cells. (A) HitPredict database predicted proteins interacting with PRMT1 with the score no less than 0.65. (B) RNA pull down assay monitored the binding affinity of PRMT1 to different proteins in PC3 cells. (C) IF analyzed the co-localization of PRMT1 and ILF3 in PC3 cells. (D) GST-pull down tested the interaction of PRMT1 with different parts of ILF3 in PC3 cells. (E-F) qRT-PCR and Western blot

detected the impact of PRMT1 on ILF3 mRNA and protein levels in PC3 cells. (G) Western blot monitored changes in ILF3 protein levels in PC3 cells under different treatments. (H) Western blot detected the impact of PRMT1 on the methylation of ILF3 WT or ILF3 R609K. (I) CoIP analyzed changes in the methylation of ILF3 WT and ILF3 R609K in PC3 cells with or without PRMT1 overexpression.

Fig. 4 ILF3 binds to and stabilizes IL-8 mRNA in PCa cells. (A) StarBase predicted the interaction between ILF3 and IL8 mRNA. (B-C) RIP and RNA pull down experiments verified the interaction between ILF3 and IL8 mRNA. (D-E) qRT-PCR and Western blot tested the impact of ILF3 silence on IL8 expression. (F-G) Luciferase reporter assays analyzed the influence of ILF3 overexpression on the activity of IL-8 promoter or IL-8 3'UTR. (H) qRT-PCR analyzed the degradation of IL-8 or ACTB mRNA in ILF3-silenced PC3 cells under ActD treatment for indicated times. $^{**}P<0.01$.

Fig. 5 Circ_0094606 accelerates M2 polarization of macrophages in PCa. (A-B) Flow cytometry analyzed the percentage of $CD14^{+}CD206^{+}$ M2 macrophages or $CD14^{+}CD86^{+}$ M1 macrophages under co-culture of circ_0094606-silenced PC3 cells. (C) qRT-PCR tested the expression of M2 markers including IL4, CCL22 and ARG1 in macrophages after co-cultured with different PC3 cells. (D) qRT-PCR tested the expression of M1 markers including iNOS, TNF-α and TLR4 in macrophages after co-cultured with different PC3 cells. (E) Western blot detected the protein levels of M1/M2 markers under indicated conditions. (F-G) qRT-PCR and Western blot analyzed the impact of circ_0094606 on IL-8 expression in PC3 cells. $^{**}P<0.01$.

Fig. 6 Circ_0094606 promotes tumorgenesis and macrophages M2 polarization in vivo. (A) The growth curves of tumors generated from PC3 transfected with NC or sh-circ_0094606. (B) Images of tumors from different groups. (C) Tumor weights in indicated groups. (D) IHC tested Ki67 staining in indicated tumors. (E) Western blot examined EMT-associated proteins in indicated tumors. (F) Western blot examined ILF3 and IL-8 levels in these tumors. (G) Flow cytometry analyzed the proportion of M2 and M1 macrophages in tumors. (H) Western blot tested the expression level of M1/M2 markers of indicated groups. $^{**}P<0.01$.

Figure 1

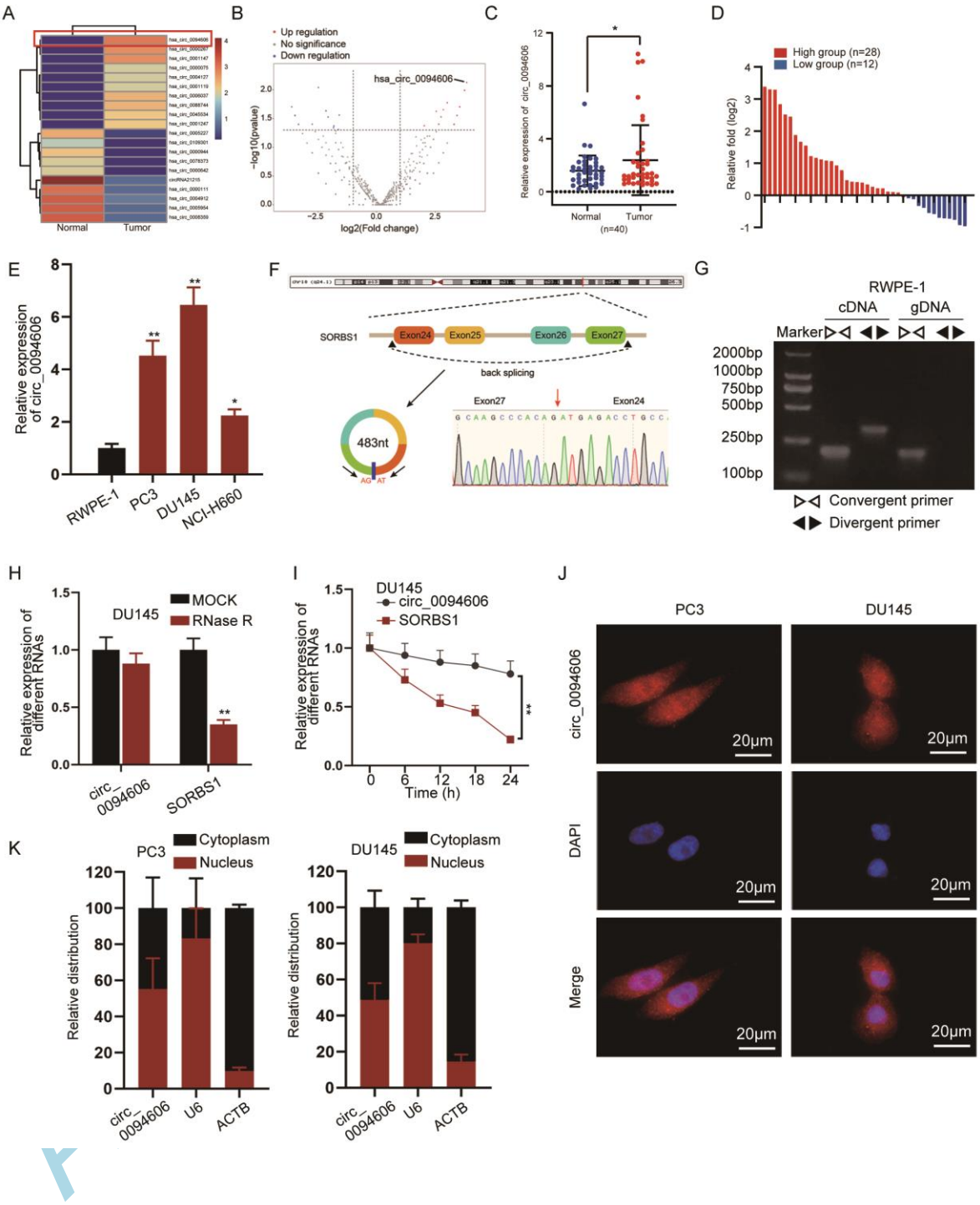

Figure 2

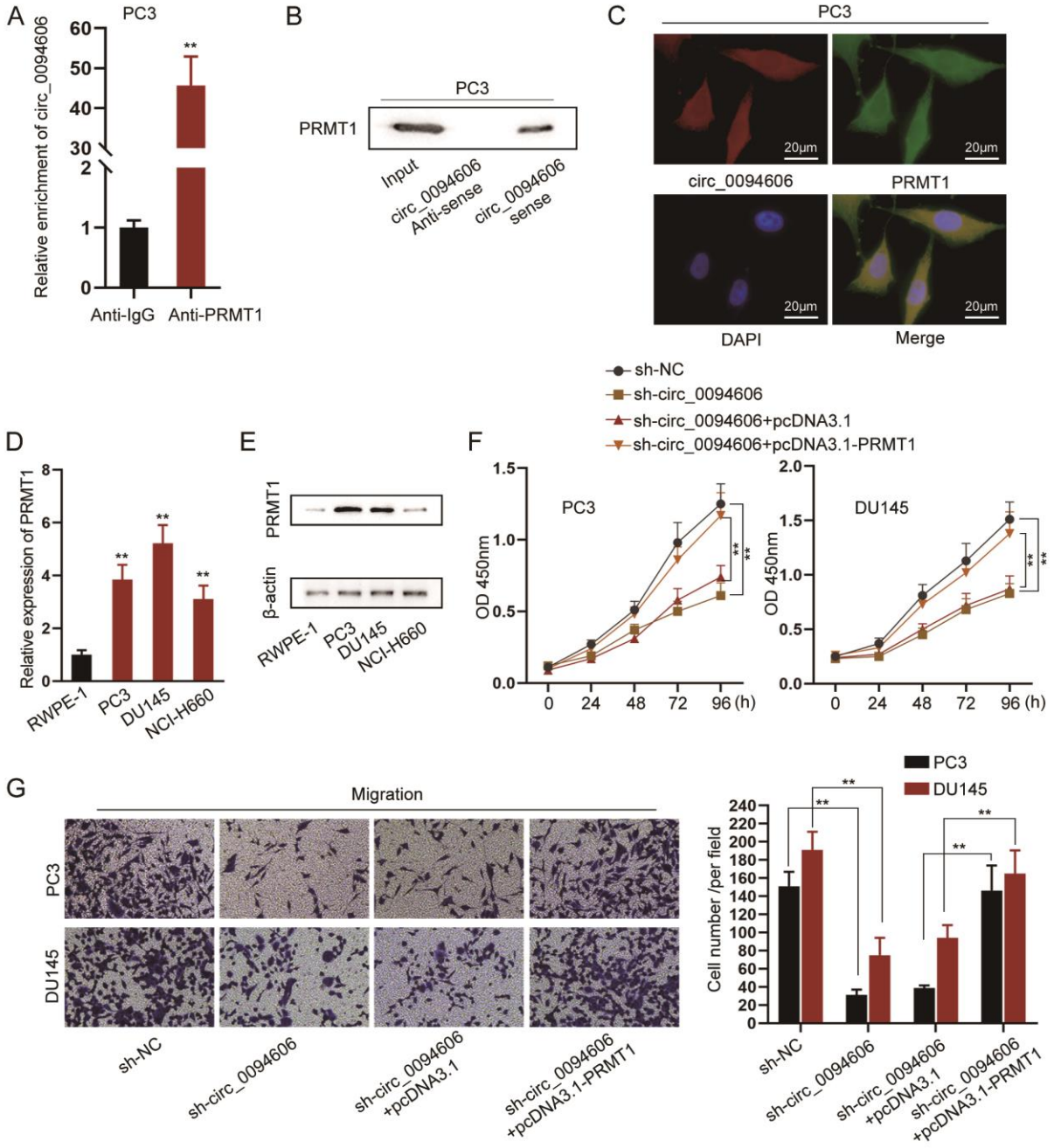

Figure 3

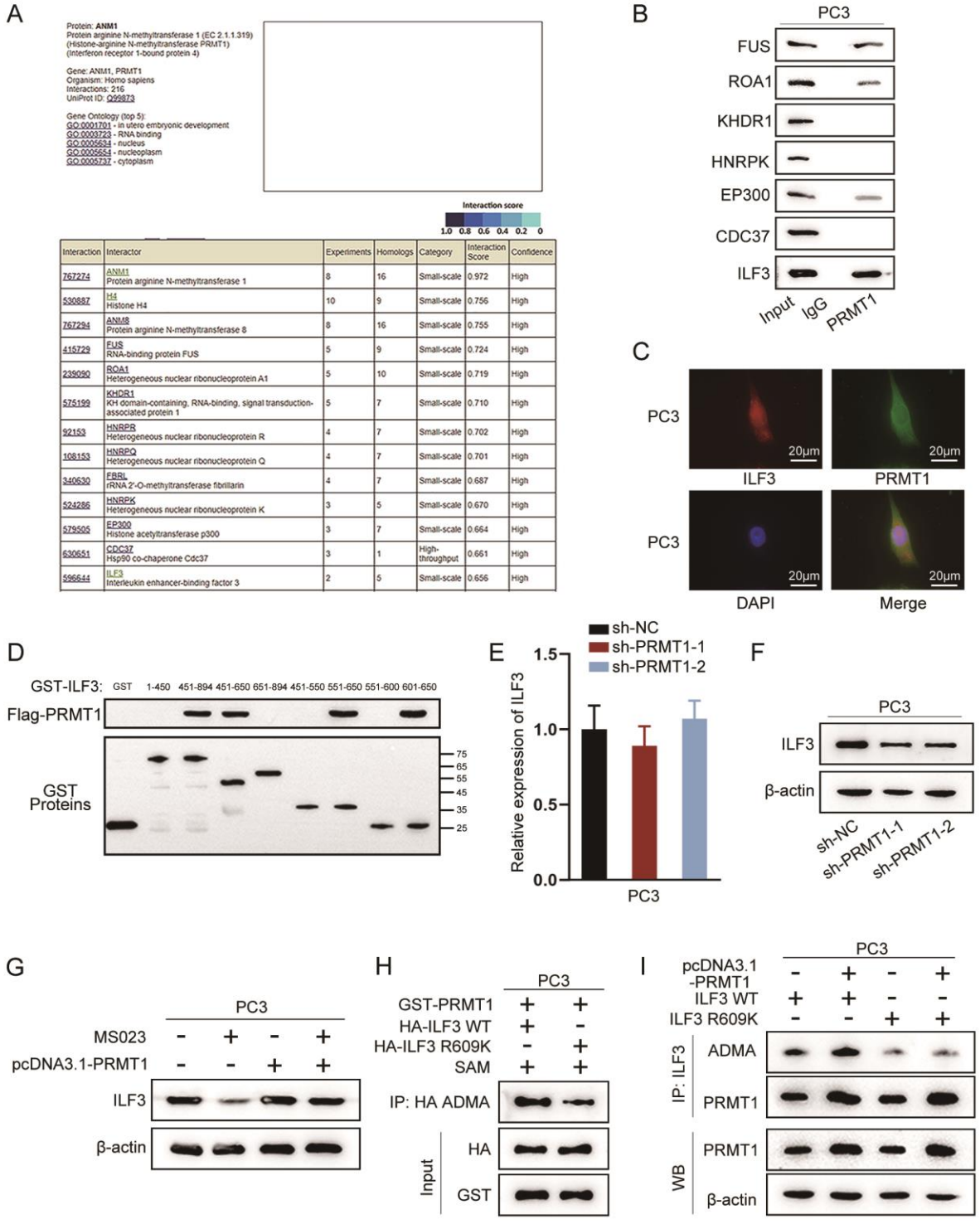

Figure 4

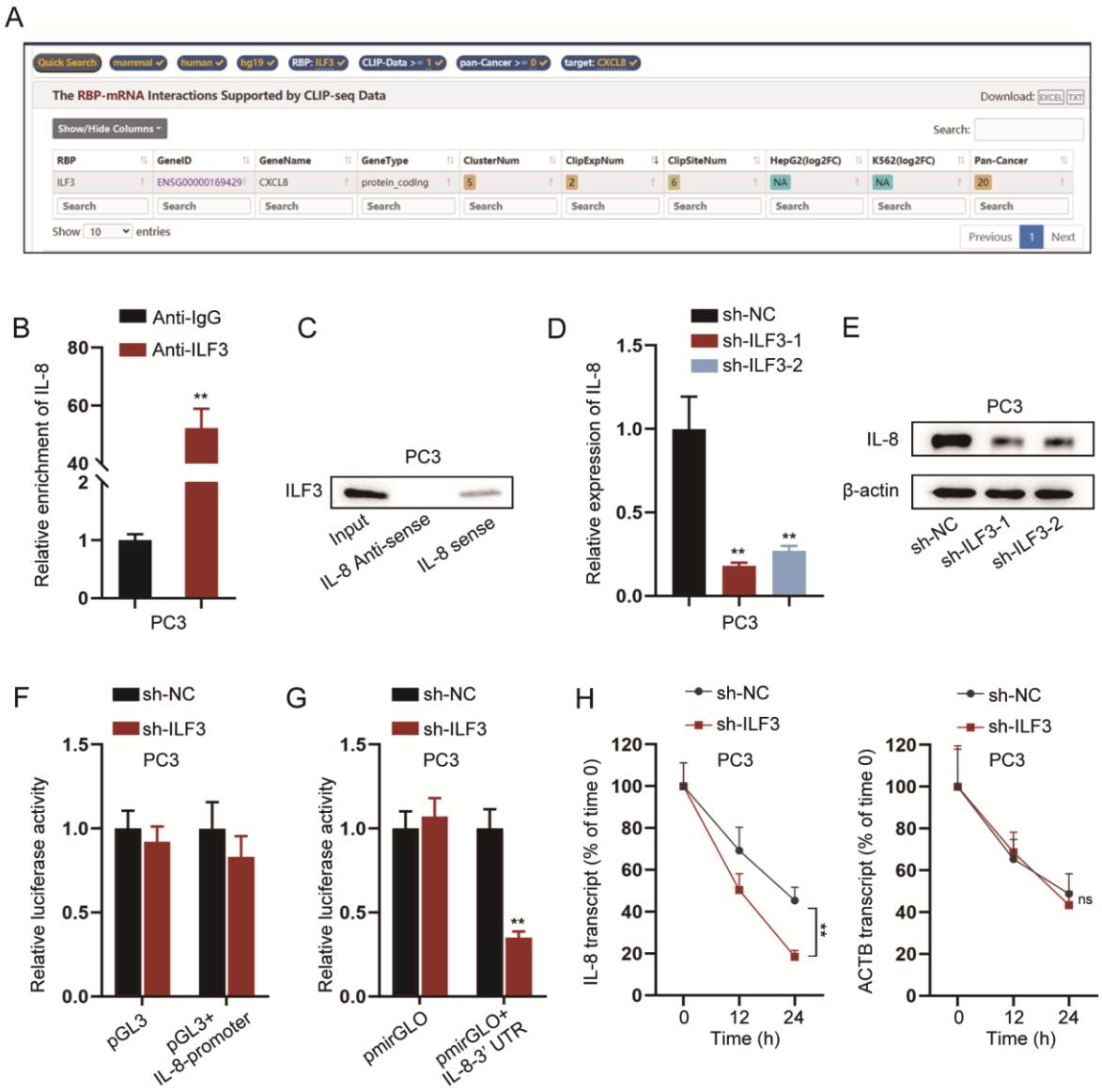

Figure 5

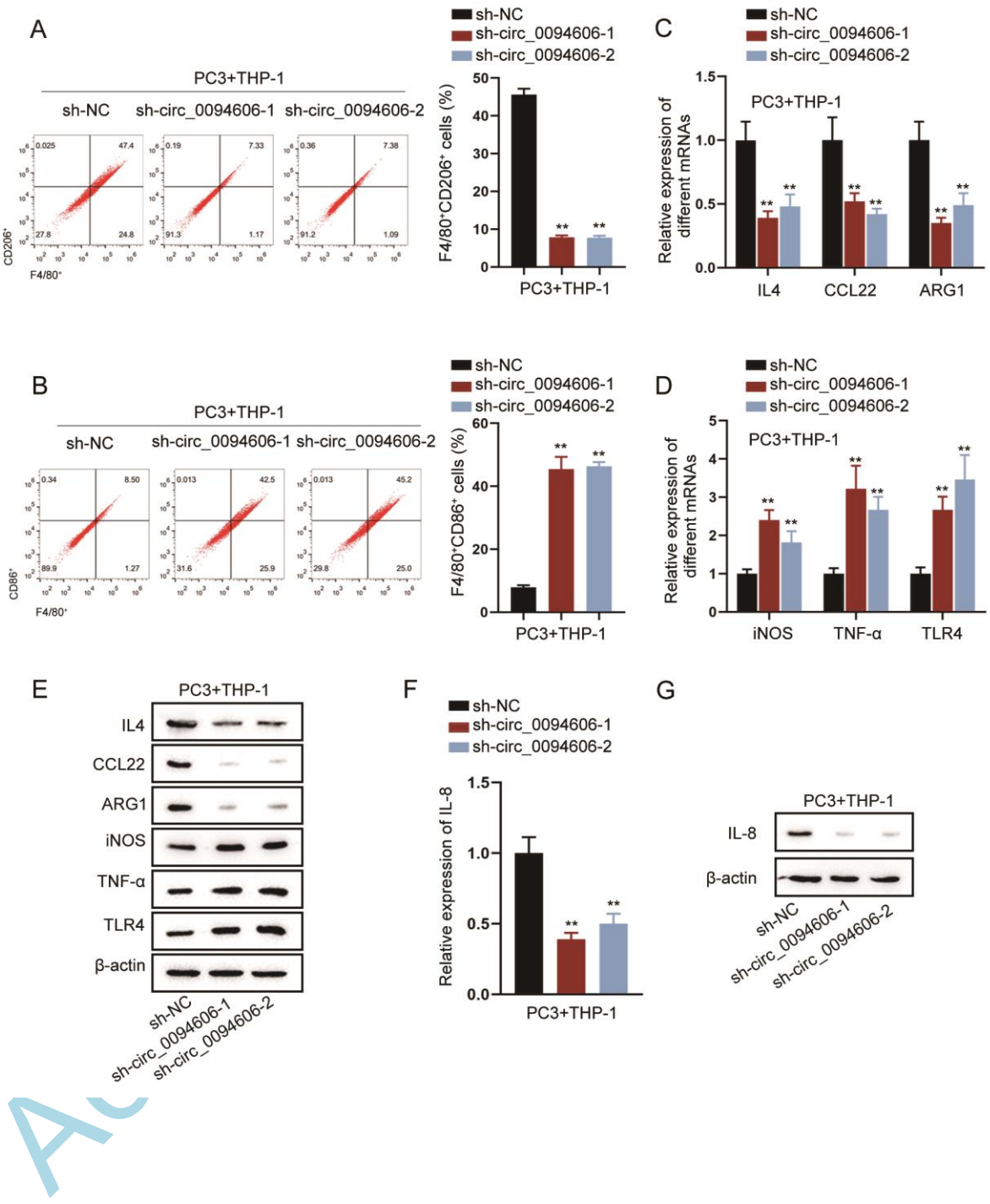

Figure 6